IJCTA, 10(02), 2017, pp. 183-194

Fault Classification and Location of an UPFC-Compensated Transmission Line using Extreme Learning Machine

M. Karthikeyan* and R. Rengaraj**

Abstract : Distance protection of transmission lines, including unified power flow controller (UPFC), has been a challenging task. This article presents a novel approach for the protection of UPFC-compensated line using extreme learning machine (ELM). The proposed method is able to classify and locate the fault in an UPFC-compensated power transmission line. The samples of three-phase line currents for half cycle duration are used to complete this task. The robustness of the proposed method has been tested with 18560 fault cases with variation in parameters on a 300-km, 735-kV line with UPFC placed in the midpoint of the line. The proposed method is simple, reliable, effective and accurate in fault classification and location of UPFC compensated transmission line.

Keywords : UPFC, Discrete wavelet transform, Extreme learning machine.

1. INTRODUCTION

The power transfer capability of existing transmission lines can be improved by using flexible ac transmission system (FACTS) devices. FACTS devices can be used to alter power system parameters to control power flow. With FACTS technology, such as static synchronous compensators (STATCOMs) and unified power flow controllers (UPFCs), bus voltages, line impedances and phase angles in the power system can be flexibly and rapidly regulated. The FACTS devices have the capability of increasing transmission capabilities, decreasing the generation cost and improving the security and stability of power system [1]. During fault, the presence of compensating devices affects steady-state and transient components of current and voltage signals that create problems with relay functionality [2- 3].

A comprehensive survey of literature indicates that different attempts have been made for fault recognition algorithms. The Kalman filtering approach has its limitation, as fault resistance cannot be modeled and furthermore it requires a number of different filters to accomplish this task [4]. The artificial neural network-based pattern recognition procedures have found wide applications for classification and location of faults in transmission line [5]. It needs large training sets and the learning process is usually consuming time. Transmission line protection using numerical methods such as wavelet transform (WT), S-transform and TT-transform have been attempted [6–8]. Support vector machines (SVMs) have been applied in power system protection [9-11] because of their high capability in classification problems. All these attempts were trying to classify the fault and identify the faulted section in a transmission line compensated by series capacitor or compensated by thyristor-controlled series compensators protected by metal-oxide varistor.

* Department of Electrical & Electronics Engineering Velammal Engineering College Chennai, India 600 066 *E-mail: eee.karthikeyan@velammal.edu.in*

** Department of Electrical & Electronics Engineering SSN College of Engineering Chennai, India 603110 *E-mail: rengarajr@ssn.edu.in*

The UPFC, which has been recognized as one of the best featured FACTS devices, is capable of providing simultaneous active and reactive power flow control as well as voltage magnitude control. The UPFC is a combination of STATCOM and static synchronous series compensator (SSSC), which are connected via a common DC link to allow bidirectional flow of real power between series output terminals of SSSC and the shunt terminals of the STATCOM [1]. Current and voltage signals have been used to determine the fault location [12]. For fault occurring behind the series capacitor (as observed from relaying point), the voltage across the series capacitor is estimated, which is subsequently subtracted from the voltage drop in the line. On the other hand, for faults occurring before the capacitor (as observed from relaying point), the voltage measured by the relay represents the voltage drop in the line, and hence, this voltage is used to calculate the voltage phasor. Although this method is conceptually simple, it requires the knowledge of fault zone (whether before or after the capacitor). However the proposed method uses only the current samples to classify and locate the fault.

2. PROPOSED METHOD FOR FAULT CLASSIFICATION AND LOCATION

The proposed method uses fault current signal samples after the fault inception at the relay location. Discrete wavelet transform (DWT) is used to extract the attributes from the sampled version of the three line currents. For this purpose, samples for the duration of only half cycle have been used. The detailed coefficients of the three phase currents are extracted by DWT and these coefficients are provided at the input to ELM, which classifies and locates the fault. The output of the fault classifier is the fault type. The output of the fault locator is the distance in kilometer from the relay location. The flow chart of the proposed method is shown in Fig. 1.

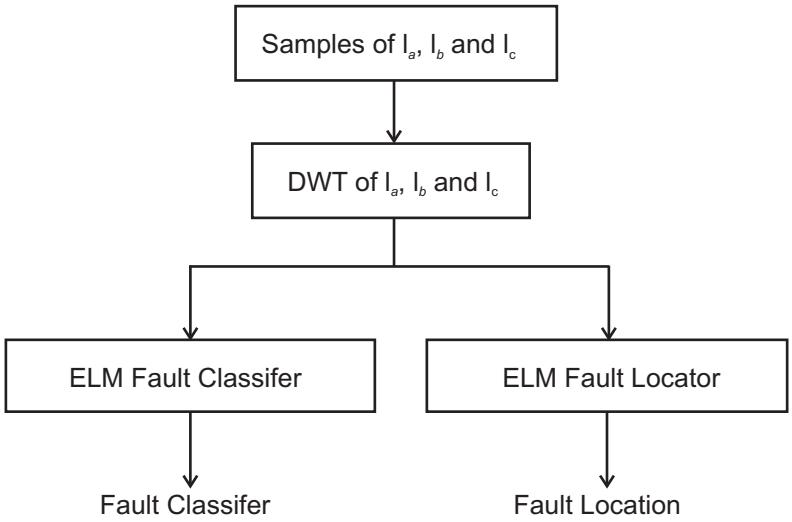

Figure 1: Flowchart for the proposed method

3. WAVELET TRANSFORM

Wavelet transform (WT) is a signal processing tool that performs time localization of different frequency components of a given signal. Therefore, by using wavelet transform, both time and frequency resolutions of the given current signal are accomplished. WT performs this task by using some unique analyzing functions called mother wavelets. The unique property of the mother wavelet is that for high-frequency components, the time intervals would be short, whereas for low-frequency components, the time intervals would be longer. The definition of Continuous wavelet transform (CWT) for a given fault current signal $i(t)$ with respect to mother wavelet $\psi(t)$ is,

$$\mathrm{CWT}(a, b) = \frac{1}{\sqrt{a}} \int_{-\infty}^{+\infty} i(t)\psi\left(\frac{t-b}{a}\right) dt \tag{1}$$

where, a is the scale factor and b is the translation factor. Discrete wavelet transform can be written as

$$\text{DWTT}(m, n) = \frac{1}{\sqrt{a_o^m}} \sum_k i(k) \psi \left(\frac{n - k b_o a_o^m}{a_o^m} \right) \tag{2}$$

where, a and b parameters in (2) are changed to be the functions of integers m, n and k, which is an integer variable and it refers to a sample number in the input fault current signal. Generally, DWT is implemented through multi resolution analysis (MRA). A schematic diagram of MRA is shown in Figure 2.

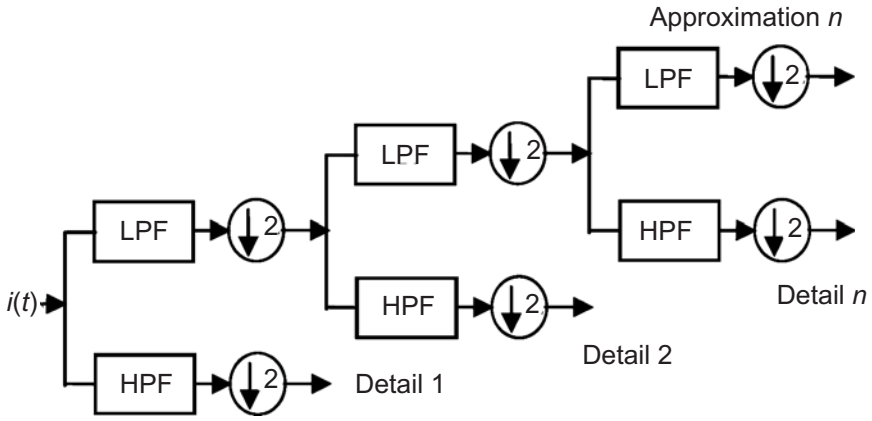

Figure 2: Schematic diagram of MRA

In the first stage, the original fault current signal $i(t)$ is decomposed into two halves of frequency components by using high-pass filter (HPF) and low-pass filter (LPF). In the second stage, the output of the LPF is sent again to another set of HPF and LPF to further decompose the current signal into two halves of frequency components. This process is repeated till the desired level of decomposition of the original current signal is achieved. If the sampling frequency of the original signal is f_s, then as per the sampling theorem, the highest frequency component that the signal could contain is $f_s/2$. Hence, in the first level, the band of frequencies between $f_s/2$ and $f_s/4$ would be captured. In the second level, the band of frequencies between $f_s/4$ and $f_s/8$ would be captured and so on [13].

WT is useful in analyzing the transient phenomena associated with transmission line faults. This technique can be used effectively for realizing nonstationary fault current signals comprising of high and low-frequency components, through the use of a variable window length of the fault current signal. The ability of the WT to focus on short-time intervals for high-frequency components and long-time intervals for low-frequency components improves the analysis of transient signals. For this reason, wavelet decomposition is ideal for studying transient signals and obtaining better current characterization and a more reliable discrimination is achieved.

A. Selection of mother wavelet

The choice of mother wavelet plays a major role in the characterization of the current signal under study. The mother wavelet, whose characteristics matches closely with the signal under consideration, would be the best choice. The mother wavelet should have enough number of vanishing moments to represent the salient features of the disturbances. The mother wavelet should provide sharp cut-off frequencies to reduce the amount of leakage energy to the adjacent resolution levels. The mother wavelet should obtain higher total energy of the same feature of the same signal. The minimum description length (MDL) data criterion is applied to select the optimum wavelet function. Since Daubechies wavelet functions have the smallest MDL indices, it has been selected as the mother wavelet in this work [14]. Based on extensive simulation studies carried out, Daubechies8 (db8) wavelet is chosen in this case.

B. Selection of decomposition level

A higher decomposition level is used in order not to miss the features of current signal. Once a mother wavelet is selected the data independent selection (DIS) method is considered to determine the optimal levels of decomposition [15]. The number of decomposition levels (n_{LS}) is given by

$$n_{LS} = \text{floor}\left(\frac{\log(f_s / f)}{\log 2}\right) \tag{3}$$

where floor() means to take integral part of the calculation result. f_s is the sampling frequency and f is the fundamental frequency of the current signal.

4. EXTREME LEARNING MACHINE

In a single layer feedforward network (SLFN), it is possible to fix the weights between input neurons and hidden neurons. The weights between hidden neurons and output neurons can be adjusted. On the basis of this, Guang-Bin Huang et al. (2006) proposed a new learning algorithm referred to as extreme learning machine (ELM). ELM randomly chooses and fixes the weights between input neurons and hidden neurons based on some continuous probability density function and then analytically determines the weights between hidden neurons and output neurons of the SLFN.

A. Approximation problem of SLFNs

For N samples $\{(x_k, t_k)\}_{k=1}^{N}$, where $x_k = [x_{k1}, x_{k2}, ...,x_{kn}]^T$ and $t_k = [t_{k1}, t_{k2}, ..., t_{kn}]^T$ a standard SLFN with $\tilde{N}$ hidden neurons and activation function $g(x)$ is mathematically modeled as:

$$\sum_{i=1}^{\tilde{N}} \beta_i g(w_i \cdot x_k + b_i) = O_k, \; k = 1, 2, ..., N \tag{4}$$

where, $w_i = [w_{i1}, w_{i2}, ..., w_{in}]^T$ is the weight vector connecting the i^{th} hidden neuron and the input neurons, $\beta_i = [\beta_{i1}, \beta_{i2}, ..., \beta_{in}]^T$ is the weight vector connecting the i^{th} hidden neuron and the output neurons, $O_k = [O_{k1}, O_{k2}, ..., O_{kn}]^T$ is the output vector of the SLFN and b_i is the threshold of the i^{th} hidden neuron. $w_i \,.\, x_k$ denotes the inner product of w_i and x_k. These N equations can be written compactly as:

$$H\beta = O \tag{5}$$

where,

$$H = \begin{bmatrix} g(w_1 \cdot x_1 + b_1) & \cdots & g(w_{\tilde{N}} \cdot x_1 + b_{\tilde{N}}) \\ \vdots & \cdots & \vdots \\ g(w_1 \cdot x_N + b_1) & \cdots & g(w_{\tilde{N}} \cdot x_N + b_{\tilde{N}}) \end{bmatrix}_{N \times \tilde{N}} \tag{6}$$

$$\beta = \begin{bmatrix} \beta_1^T \\ \vdots \\ \beta_{\tilde{N}}^T \end{bmatrix}_{\tilde{N} \times m} \tag{7}$$

and

$$O = \begin{bmatrix} O_1^T \\ \vdots \\ O_N^T \end{bmatrix}_{N \times m} \tag{8}$$

Here, H is called the hidden layer output matrix.

B. ELM learning algorithm

The number of hidden neurons required to achieve a good generalization performance is much less. The resulting training error might not approach to zero but can be minimized by solving the following problem:

$$\min_{\beta} \left\| \mathrm{H}(w_1,...,w_{\tilde{N}},b_1,...,b_{\tilde{N}})\beta - \mathrm{T} \right\|^2 \tag{9}$$

where,

$$\mathrm{T} = \begin{bmatrix} t_1^{\mathrm{T}} \\ \cdot \\ \cdot \\ \cdot \\ t_{\mathrm{N}}^{\mathrm{T}} \end{bmatrix}_{\mathrm{N}\ \mathrm{X}\ m} \tag{10}$$

ELM randomly assigns and fixes the input weights w_i and biases b_i based on some continuous probability distribution function in the case of learning a structured function, only leaving output weights β_i to be adjusted according to:

$$\min_{\beta} \left\| \mathrm{H}\beta - \mathrm{T} \right\|^2 .$$

The above problem is linear system optimization problem. Its unique least-squares solution with minimum norm is given by

$$\hat{\beta} = \mathrm{H}^{\dagger}\mathrm{T} \tag{11}$$

where, $\mathrm{H}^{\dagger}$ is the Moore-Penrose generalized inverse of matrix H. The solution produced by ELM in Equation(11) not only achieves the minimum square training error but also the best generalization performance on novel patterns.

C. ELM Algorithm

Given a training set $\mathrm{N} = \{(x_i,t_i) \mid x_i \in \mathrm{R}^n,\ t_i \in \mathrm{R}^m, i = 1,...,\mathrm{N}\}$, activation function $g(x)$, and hidden node number L, the algorithm is represented by the following steps:

Step 1: Randomly assign input weight w_i and bias b_i, i = 1,...L

Step 2: Calculate the hidden layer output matrix H.

Step 3: Calculate the output weight β

$$\hat{\beta} = \mathrm{H}^{\dagger}\mathrm{T},$$

where

$$\mathrm{T} = [t_1, \ldots t_{\mathrm{N}}]^{\mathrm{T}}. \tag{11}$$

ELM can perform direct classification for multi-category problems in a fast and efficient manner. Many non-linear activation functions can be used in ELM, like sigmoid, sine, hard limit, radial basis functions, and complex activation functions. The activation functions used in ELM may be non differentiable or even discontinuous [16-18].

5. TEST SYSTEM

The proposed method has been tested on a 735-kV, 50-Hz power system consisting of two sources representing two area (Area1, Area2) connected by a tie line (T.L.1, T.L.2) of 300 km with UPFC placed at the middle of the line. The transmission line model chosen for this work is of distributed type. The test system is shown in Fig. 3. It also contains two transformers (Trans1, Trans2), Loads (L_1, L_2, L_3, L_4, L_5). B_1, B_2, B_3, B_4, B_5 are the bus to which the components of the test systems are connected. The test system data are listed in Appendix. The Simulation model is developed using MATLAB-SIMULINK environment. The simulation frequency is 1.25 kHz based on simulation studies.

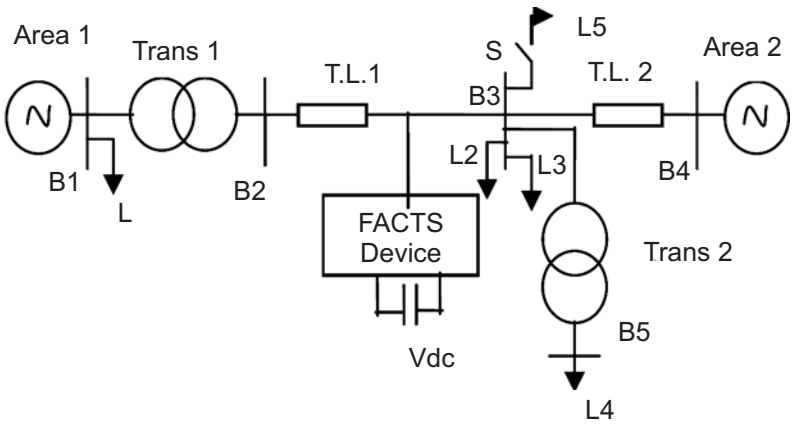

Figure 3: One line diagram of the test system

6. SIMULATION RESULTS

Sample waveforms of three phase currents for a single line to ground fault before and after UPFC is shown in Fig.4 and Fig.6. Approximation and details of the faulted phase A current is shown in Fig.5 and Fig.7.

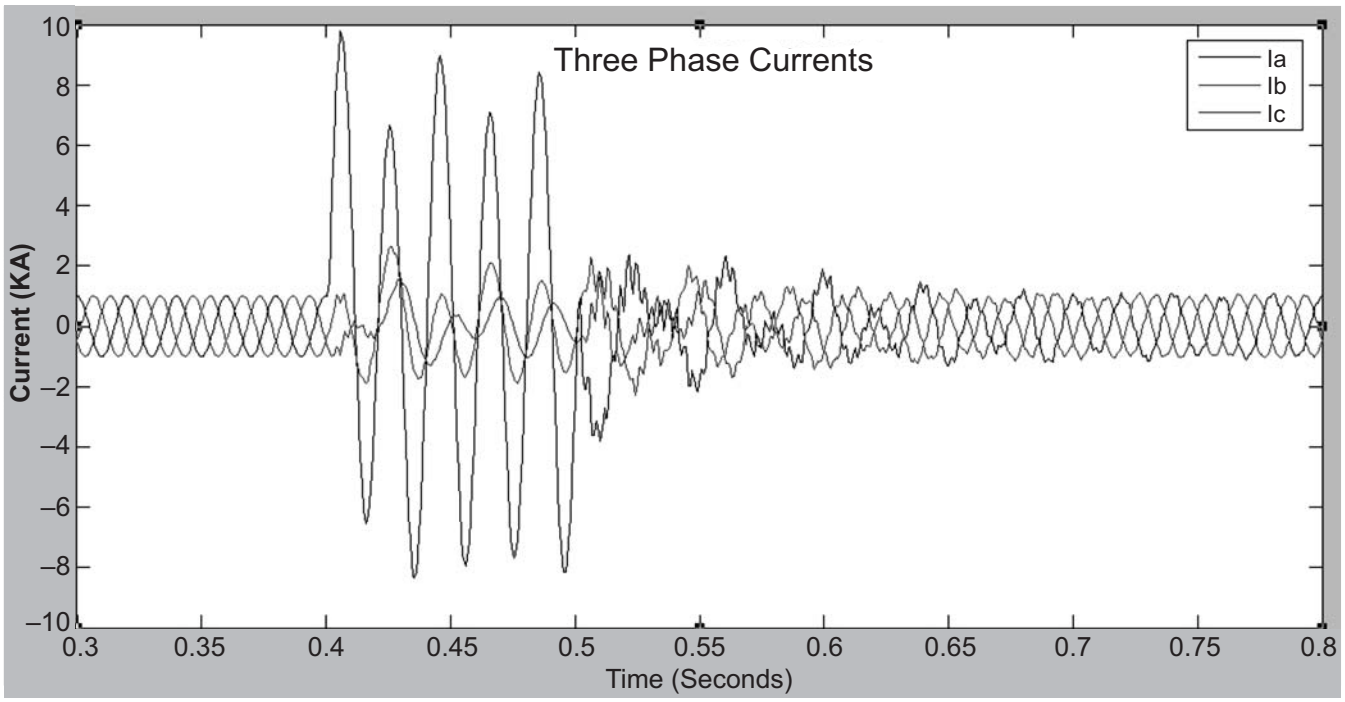

Figure 4: Three phase current waveforms during single line to ground fault before UPFC

7. FAULT CLASSIFICATION

To study the effectiveness of the proposed method under different system conditions, different combinations of source impedances (Z_{S1} & Z_{S2}) have been considered. For fault classification, the fault simulation studies have been performed under wide variation of fault resistance (R_f), fault location (E), fault inception angle(FLA), and load angle(δ). The parameter values that have been chosen for training are shown in Table 1. The training patterns are generated for ten different types of fault (A-G, B-G, C-G, A-B, B-C, A-C, A-B-G, B-C-G, A-C-G and A-B-C) on the transmission line with 3 source impedances, 2 locations, 2 fault resistances, 2 fault inception angles and 2 load angles. Thus a total of $10 \times 3 \times 2 \times 2 \times 2 \times 2 = 480$ cases have been generated for training. The duration of the fault has been assumed to be five cycles.

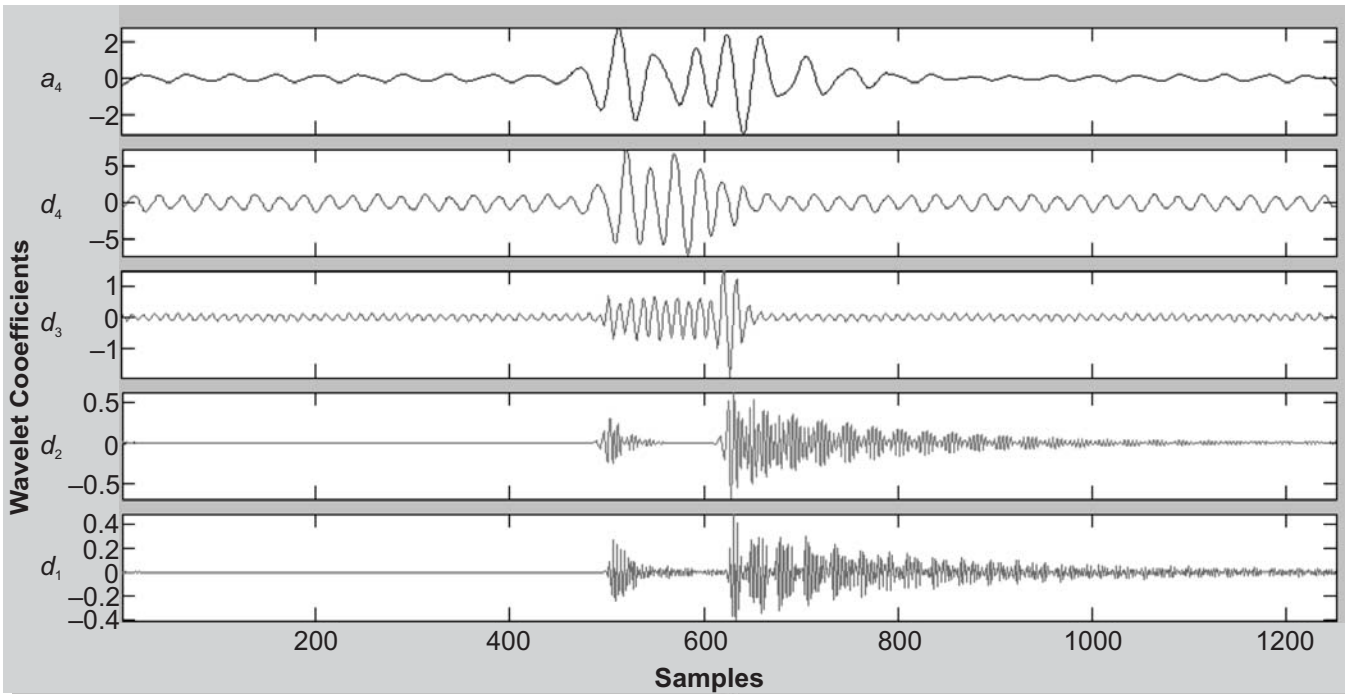

Figure 5: Wavelet coefficients of phase A during single line to ground fault before UPFC

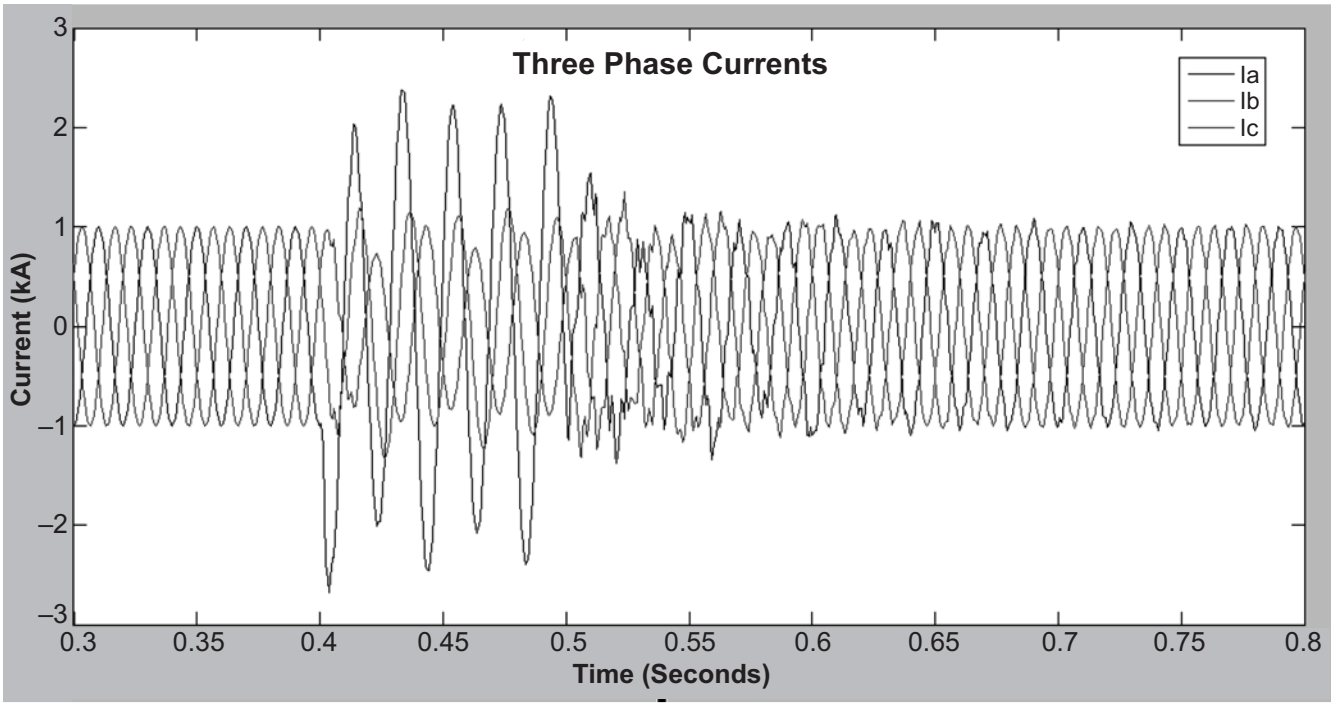

Figure 6: Three phase current waveforms during single line to ground fault after UPFC

To test the effectiveness of the proposed method, the fault simulation studies have been performed under wide variation of system parameters. The parameter values that have been chosen for testing are shown in Table II. The testing patterns are generated for ten different types of fault on the transmission line with 5 source impedances, 4 locations, 4 fault resistances, 4 fault inception angles and 3 load angles. Thus, a total of $10 \times 5 \times 4 \times 4 \times 4 \times 3 = 9600$ cases have been generated for testing.

In this article, ELM is used as a pattern classifier. ELM supports the multi-class classification. The half cycle fault current samples after pre-processing using DWT are taken as input to the classifier. The training and test patterns are normalized to [-1 1]. For accurate fault classification, the classifier is trained

with 480 fault cases as described above. After the classifier is trained, its performance has been tested with 9600 fault cases, which are not part of training set.

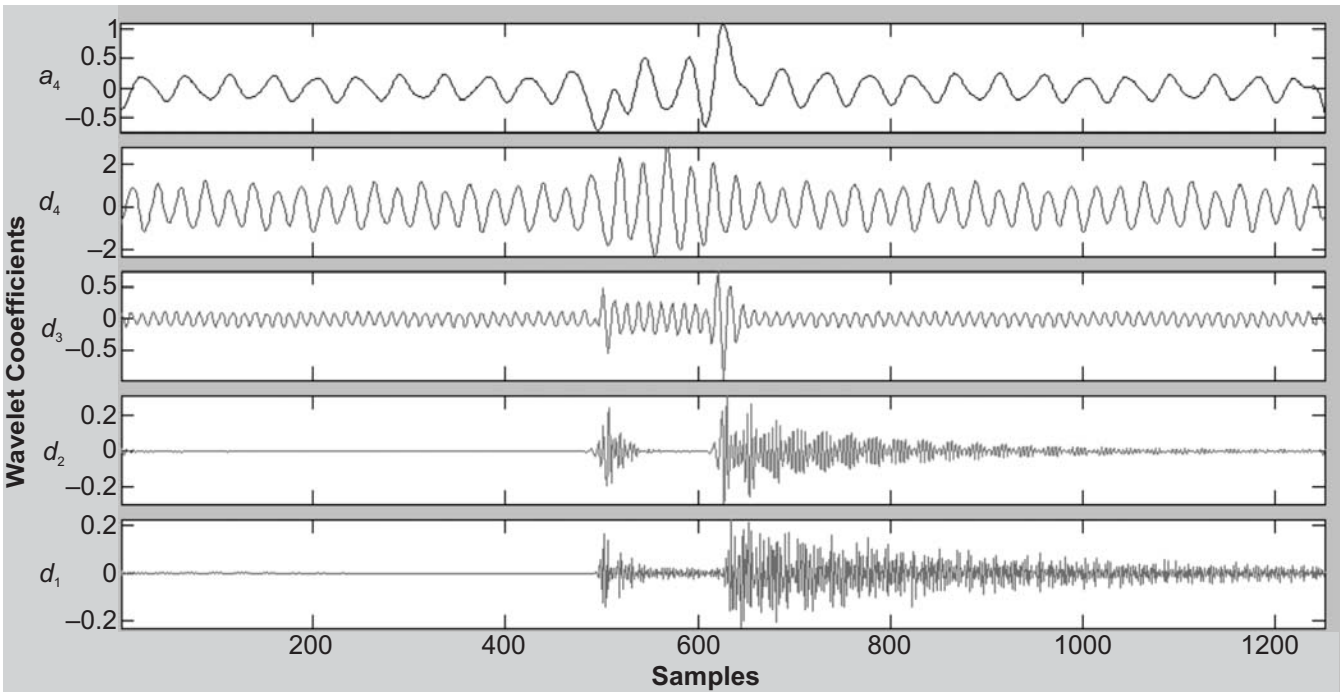

Figure 7: Wavelet coefficients of phase A during single line to ground fault after UPFC

Table 1

Cases Considred for Dataset Generation

Case No.	*No of fault cases*	*Training Parameters*					
		Z_{S1} *(%)*	Z_{S2} *(%)*	*E*	R_f	*FLA*	δ
1.	160	100	100	40%, 80% of Line Length	50Ω, 100Ω	0º, 90º	10º, 30º
2.	160	75	75				
3.	160	125	125				
Total training data cases = 160 x 3 = 480							

Table 2

Cases Considered for Testing Dataset Generation

Case No.	*No of fault cases*	*Testing Parameters*					
		Z_{S1} *(%)*	Z_{S2} *(%)*	*E*	R_f	*FIA*	δ
1.	1920	100	100	30%, 45%, 60%, 75% of Line Length	1Ω, 50Ω, 150Ω, 200Ω	36º, 72º, 108º, 120º	10º, 30º, 60º
2.	1920	100	75				
3.	1920	75	100				
4.	1920	100	125				
5.	1920	100	100				
Total testing data cases = 1920 x 5 = 9600							

8. FAULT LOCATION

The training patterns are generated by simulating the four types of fault (LG, LL, LLG and LLL) at different locations (starting from 5 km with increment of 10 km) on the transmission line from the relay location. Overall, the training patterns are generated for each type of fault on the transmission line over 28 different locations with 2 fault resistances, 2 source impedances, 2 load angles, and 2 fault inception angles. For each type of fault, the number of training patterns is $28 \times 2 \times 2 \times 2 \times 2 = 448$ patterns.

The testing patterns are generated for each type of fault on the transmission line over 28 locations with 10 fault resistances, 2 source impedances, 2 fault inception angles and 2 load angles. For each type of fault, the number of testing pattern for fault location is $28 \times 10 \times 2 \times 2 \times 2 = 2240$ patterns. Thus, a total of 4 x 2240 = 8960 cases have been generated for testing. The parameter values that have been chosen for training and testing are shown in Table 3.

Table 3
Paremeters Considered for Training and Testing Dataset Generation

Parameters	*Training*	*Testing*
Fault location	05, 15, 25, 35, …, 295km	10, 20, 30, 40, …, 290 km
Fault resistance	1Ω, 10Ω	1Ω – 200Ω
Fault Inception angle	0º, 90º	0º – 120º
Load angle	10º, 30 º	20º – 60º
Source Impedance	100%, 125%	40% –125%

The structure of fault locator consists of four regression blocks as shown in Figure 8. The pre-processed fault current signals are used to train ELM fault locators. The training and test patterns are normalized to [-1 1] and given as input to the fault locator modules. In this case, the target value of each pattern is the distance from relay locations.

The criterion for evaluating the performance of the fault locator is defined as

$$\% \text{ error} = \frac{\left|\text{Fault locator output} - \text{Actual fault location}\right|}{\text{Total length of the line}} \times 100 \quad (2)$$

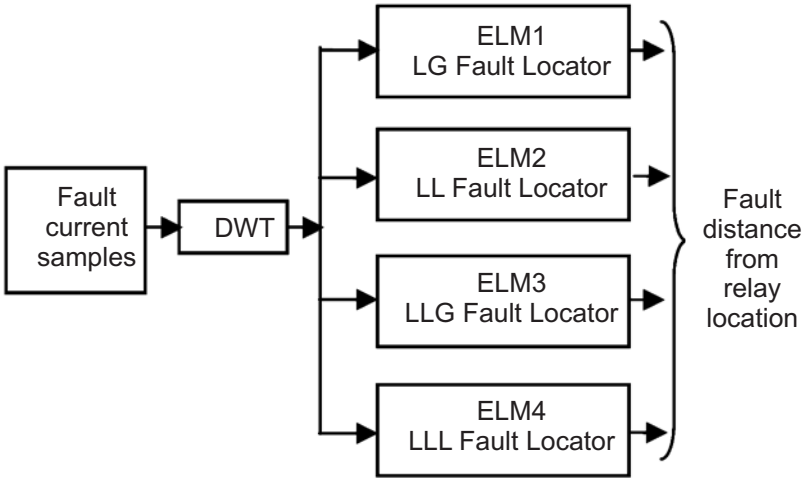

Figure 8: Block diagram representation of the fault locator for estimation of fault distance from relay location

A. Parameter selection of ELM

Based on the studies carried out, the sigmoid activation function has been used for training and testing of ELM classifier. For ELM classifier, the numbers of hidden neurons are gradually increased by 1 and optimal number of hidden neurons for ELM classifier is then selected based on training accuracy. The number of hidden neurons for fault classifier is 28. For ELM fault locator, the numbers of hidden neurons are gradually increased by 1 till the root mean square error (RMSE) is less than 0.01. The number of hidden neurons for LG, LL, LLG, LLL fault locators is 12, 18, 15, and 19 respectively.

9. RESULTS AND DISCUSSION

The classification results during testing are shown in Table 4. The diagonal elements represent correctly classified faults. Off-diagonal elements represent the misclassification. A few misclassified test patterns of WT-ELM is shown in Table 5. As observed from Table 6, the overall accuracy for fault classification with WT-ELM is 97.47%

Table 4
Classification Results of WT-ELM

Type of fault	*WT-ELM*			
	LG	*LL*	*LLG*	*LLL*
LG	2820	–	60	–
LL	–	2847	18	15
LLG	54	46	2780	–
LLL	–	40	10	910

Table 5
Samples of Misclassified Test Cases of WT-ELM

Type of Fault	Z_{S1} *(%)*	Z_{S2} *(%)*	*E (%)*	R_f	*FIA*	δ	*Classifier Output*
LG	75	100	30	200Ω	72°	60°	LLG
LL	100	125	75	150Ω	108°	30°	LLG
LLG	100	75	60	1 Ω	36°	10°	LG
LLL	100	100	45	1 Ω	72°	60°	LL

Table 6
Fault Classifier Accuracy

Type of fault	*Samples tested*	*WT-ELM*	
		True classification	*% Accuracy*
LG	2880	2820	97.92
LL	2880	2847	98.85
LLG	2880	2780	96.53
LLL	960	910	94.79
Total	9600	9357	97.47

% error distribution for ELM fault locators are given in Table 7. As observed from Table 7, ELM fault locators predicted the fault location with less than 0.5% error for 7155 test samples (80% of test data).

Table 7

% Error Distribution for ELM Fault Locatos

% error Range	*Number of test samples*				*Total test samples*
	ELM-LG fault locator	*ELM-LL fault locator*	*ELM-LLG fault locator*	*ELM-LLL fault locator*	
0.0-0.1	831	247	641	303	2022
0.1-0.2	389	244	472	436	1541
0.2-0.3	363	498	401	456	1718
0.3-0.4	230	367	252	307	1156
0.4-0.5	165	246	161	146	718
0.5-0.6	100	197	99	150	546
0.6-0.7	48	121	76	113	358
0.7-0.8	57	139	62	107	365
0.8-0.9	39	111	48	114	312
0.9-1.0	18	70	28	108	224

The minimum, maximum, mean error and standard deviation for different ELM locators are given in Table 8. As observed from Table 8, the mean error and standard deviation of ELM locators are less.

Table 8

Fault Location Error of ELM Fault Locators

Type of fault	*Min. Error*	*Max. Error*	*Mean Error*	*Standard deviation*
LG	4.0929e-006	0.9848	0.2304	0.2030
LL	3.1330e-004	0.9909	0.3830	0.2433
LLG	1.8239e-005	0.9975	0.2569	0.2217
LLL	0.0013	0.9916	0.3608	0.2505

10. CONCLUSION

In this paper, a method to classify and locate fault in an UPFC-compensated transmission line using extreme learning machine has been proposed. The detailed coefficients of the three phase currents are extracted by DWT and these coefficients are provided at the input to ELM, which classifies and locates the fault. The proposed method is tested with parameters that are not included as part of training. The effectiveness of the proposed method is tested using 18560 test cases. The overall fault classification accuracy is 97.47% using ELM. The fault locator error is less than 1% for all the four types of fault for ELM fault locators and it predicted the fault location with less than 0.5% error for 7155 test samples (80% of test data). The mean error and standard deviation of the ELM fault locator is less. Hence, it is observed that the proposed method using ELM is accurate and robust to parameter variations for the protection of transmission line, including UPFC.

11. REFERENCES

1. B.Geethalakshmi, and P.Danajayan, " Investigation of Performance of UPFC without DC Link Capacitor," *International Journal of Electric Power System Research*, Vol. 78, No.4, pp. 736-746, April 2007.
2. P.K.Dash and S.R.Samantray, "Phase Selection and Fault Section Identification in Thyristor Controlled Series Compensated Line Using Discrete Wavelet Transform," *International Journal of Electrical Power & Energy Systems*, Vol.26, No. 9, pp. 725-732, September 2004.
3. A.I.Megahed, A.Monem Moussa and A.E.Bayoumy, "Usage of Wavelet Transform in the Protection of Series-Compensated Transmission Lines," *IEEE Transactions on Power Delivery*, Vol.21, No.3, pp.1213-1221, July 2006.

4. S.R.Samantaray, P.K.Dash and S.K.Upadhyay, "Adaptive Kalman Filter and Neural Network Based on High Impedance Fault Detection in Power Distribution Networks," *International Journal of Electrical Power & Energy Systems,* Vol.31, No.4, pp.167-172, May 2009.
5. Song YH, Johns AT, Xuan QY, "Artificial Neural Network Based Protection Scheme for Controllable Series Compensated EHV Transmission Line," *IEE Generation, Transmission and Distribution*, Vol.143, pp.535-540, 1996
6. S.R.Samantaray, P.K.Dash, "Pattern Recognition Based Digital Relaying for Advanced Series Compensated Line," *International Journal of Electrical Power & Energy Systems*, Vol.30, No.1, pp.102-112, February 2008.
7. Osman A.H. and Malik O.P., 'Transmission line protection based on wavelet transform', *IEEE Trans. Power Delivery*, Vol.19, No.2, pp.515-523, April 2004.
8. S.Suja and J.Jerome, "Pattern Recognition of Power Signal Disturbances Using S Transform and TT Transform," *International Journal of Electrical Power & Energy Systems*, Vol.32, No.1, pp.37-53, Jan. 2010.
9. P.K.Dash, S.R.Samantaray, and G.Panda, "Fault Classification and Section Identification of an Advanced Series-Compensated Transmission Line Using Support Vector Machine ," *IEEE Transactions on Power Delivery,* Vol.22, No.1, pp.67-73, January 2007.
10. Urmil B.Parikh, Biswarup Das and Rudra Prakash Maheswari, "Combined Wavelet-SVM Technique for Fault Zone Detection in a Series Compensated Transmission Line" *IEEE Transactions on Power Delivery*, Vol.23, No.4, pp.1789-1794, October 2008.
11. Urmil B.Parikh, Biswarup Das and Rudra Prakash Maheswari, "Fault Classification Technique for Series Compensated Transmission Line Using Support Vector Machine" *International Journal of Electrical Power & Energy Systems*, Vol.32, No.4, pp.629-636, May 2009.
12. J.Sadesh and A.Adinehzadeh, "Accurate Fault Location Algorithm for Transmission Line in the Presence of Series Connected FACTS Devices," *International Journal of Electrical Power & Energy Systems*, Vol.32, No.4, pp.323-328, May 2010.
13. Daubechies I. (1992), Ten lectures on wavelets, Philadelphia, Pennsylvania, SIAM.
14. W.Gao and J.Ning, "Wavelet-based disturbance analysis for power system wide-area monitoring," IEEE Trans. Smart Grid, Vo1. 2, No.1, pp.121-130, January 2011.
15. J.A.Daviu, M.Riera-Guasp, J.Roger-Folch,F.Martínez- Giménez, and A. Peris, "Application and optimization of the discrete wavelet transform for the detection of broken rotor bars in induction machines" *Appl.Comput. Harmon. Anal.*, vol. 21, no. 2, pp. 268–279, 2006.
16. Guang-Bin Huang, Qin-Yu Zhu and Chee-Kheong Siew, 'Extreme learning Machine: Theory and applications' *Neurocomputing*, Vol.70, pp.489-501, 2006.
17. Guang-Bin Huang, Qin-Yu Zhu and Chee-Kheong Siew, 'Universal approximation using incremental constructive feedforward networks with random hidden nodes', *IEEE Trans. Neural Networks*, Vol.17, No.4, pp.879-892, December 2006.
18. Guang-Bin Huang and Siew C.K., 'Extreme Learning Machine with randomly assigned RBF Kernels', *Int. J. of Information Technology*, Vol.11, No.1, pp.16-24, 2005.